




8-2014

Self-Supported Printed Multi-Layer Capacitors

Michael James Joyce
Western Michigan University

Follow this and additional works at: https://scholarworks.wmich.edu/masters_theses

 Part of the Chemical Engineering Commons, Engineering Science and Materials Commons, and the Materials Science and Engineering Commons

Recommended Citation

Joyce, Michael James, "Self-Supported Printed Multi-Layer Capacitors" (2014). *Masters Theses*. 526.
https://scholarworks.wmich.edu/masters_theses/526

This Masters Thesis-Open Access is brought to you for free and open access by the Graduate College at ScholarWorks at WMU. It has been accepted for inclusion in Masters Theses by an authorized administrator of ScholarWorks at WMU. For more information, please contact wmu-scholarworks@wmich.edu.



SELF-SUPPORTED PRINTED MULTI-LAYER CAPACITORS

by

Michael James Joyce

A thesis submitted to the Graduate College
in partial fulfillment of the requirements
for the degree of Masters of Science
Paper and Printing Science
Western Michigan University
August 2014

Thesis Committee:

Dan Fleming III, Ph.D., Chair
Alexandra Pekarovicova, Ph.D.
Massood Zandi Atashbar, Ph.D.

SELF-SUPPORTED PRINTED MULTI-LAYER CAPACITORS

Michael James Joyce, M.S.

Western Michigan University, 2014

The increasing demand for miniaturized electronic devices has increased the need for rechargeable micro-power sources. Although lithium and lithium ion batteries have been utilized in these applications since the late 1990s, other energy harvesting technologies, such as thermal, mechanical, and solar, are now being used to augment batteries to enable systems to be self-powered. However, the lifetime of any battery is finite, which may be a major problem when the application is in a permanent structure or medical implant device. For power or significant energy storage applications, printed multilayer capacitors or supercapacitors are being explored as an enhancement, or replacement of micro-batteries.

The printing of multilayer capacitors offers an inexpensive manufacturing process for these devices. Though the ability to print supercapacitor electrodes, supercapacitors, and batteries on rigid and flexible substrates has been demonstrated, the ability to print self-supported multilayer capacitors or supercapacitors has not yet been reported. This study focused on the feasibility of the fabrication and testing of self-supporting screen-printed multilayer capacitors.

Copyright by
Michael Joyce
2014

ACKNOWLEDGEMENTS

I would like to thank my advisor Dr. Dan Fleming for all his contributions to this work, and my education. Who, without his dedicated assistance and guidance this work would have not been possible. I also thank Dr. Alexandria Pekarovicova, and Dr. Massood Atashbar for all their valuable contributions and insight into this research, and the knowledge they helped me gain throughout my works.

I sincerely appreciate all the assistance provided by Mr. Matthew Stoops for his assistance in helping me to understand and use the testing equipment necessary for completion of this work. I also appreciate all the assistance from the Electrical and Computer Engineering Graduate Students (Ali Eshkeiti, Binu Baby Narakathu, Sai Guruva R Avuthu, and Sepehr Emamian) for all their contributions to my knowledge of electrical performance characterization and analysis.

I would like to thank my family, friends, and love ones for all their encouragement and support, without which, this work would have not been possible. With a special thanks to my mother Dr. Margaret Joyce, and father Dr. Thomas Joyce, for all they have done for me both for my education and personal life; without which, none of this would be possible. Lastly, I would like to give a special thanks to my future wife Emily Kinner whose love, support, and encouragement gave me the will and motivation to complete this work.

Michael Joyce

TABLE OF CONTENTS

| | |
|-------------------------------------------------|-----------|
| ACKNOWLEDGEMENTS | ii |
| LIST OF TABLES | iv |
| LIST OF FIGURES | v |
| INTRODUCTION | 1 |
| LITERATURE REVIEW | 2 |
| Capacitor and Supercapacitor Technologies | 2 |
| Lift--Off Processes | 10 |
| Overview of Printing | 11 |
| Screen---Printing | 12 |
| Problem Statement | 17 |
| EXPERIMENTAL METHODS | 18 |
| Creation of Sacrificial Layer | 18 |
| Design of Experiments..... | 19 |
| Preparation of the Alginate Films | 20 |
| Printing | 21 |
| Removal of the Sacrificial Layer | 22 |
| Analytical | 22 |
| RESULTS | 23 |
| CONCLUSIONS | 35 |
| Recommendations for Future Studies | 36 |
| REFERENCES | 38 |

LIST OF TABLES

| | |
|----------------------------------------------------------------------------|----|
| 2-1. Comparison of Conductive Inks for PE Applications ²⁸ | 7 |
| 2-2. Mesh Specifications ⁴⁹ | 15 |
| 3-1. Commercial Inks Used | 21 |
| 3-2. Screen Specifications..... | 21 |
| 3-3. Testing Equipment and Measurement Parameters..... | 23 |
| 4-1. Influence of alginate film thickness on surface energy | 23 |

LIST OF FIGURES

| | |
|--------------------------------------------------------------------------------------------------------------------------------------------------------------------------------------------------------------------------------------------------------------|----|
| 2-1. Comparison of different storage devices (Modified From Winter and Brodd) | 4 |
| 2-2. Schematic presentation of electrolytic capacitor and electrical double layer capacitor (Recreated from Jayalakshimi, 2008) | 6 |
| 2-3. Comparison of Ink Properties | 12 |
| 2-4. Comparison of Ink Film Thicknesses | 12 |
| 2-5. Schematic of Screen Printing Process (Modified from Ingram ⁴⁷ , p.2) | 13 |
| 2-6. Pictures of open and masked areas on a screen and magnified view of the emulsion layer to show the thickness of this layer | 15 |
| 3-1. Experimental Design (-)1 for alginate obtained using a #14 Meyer rod, and (+)1 obtained using a #20 Meyer rod). S-1 and D-1 refer to single layer silver and dielectric, and S+1 and D+1 refer to double layer silver and dielectric respectively. | 19 |
| 3-2. Three Layer Structure – Exploded View | 20 |
| 3-3. Three Layer Structure – Top View | 20 |
| 4-1. Molecular Structure of Sodium Alginate | 24 |
| 4-2. Dynamic Contact Angle Measurements of Alginate Films | 24 |
| 4-3. Surface roughness of the 14.41 microns alginate film | 25 |
| 4-4. Surface roughness of the 6.88 micron alginate film | 25 |
| 4-5. Variations in alginate and ink film roughness with printed and coated layers | 26 |
| 4-6. Comparison of Film Thickness Values | 27 |
| 4-7. Thinning at edges of -1D ink on +1 alginate layer due to spreading. | 28 |
| 4-8. Changes in sheet resistivity of single and double printed silver ink layers as a result of altering the thickness of the sacrificial alginate coating layer | 29 |

List of Figures-Continued

| | |
|-------------------------------------------------------------------------------------------------------------------------------------------------------|----|
| 4-9. Change in Bulk Resistivity of single and double printed Ag over alginate layers of varying thicknesses..... | 30 |
| 4-10. Comparison of the dielectric constants of single and double layer printed dielectric ink layers over alginate films of varying thicknesses..... | 31 |
| 4-11. Changes in Ink film density resulting from the printing of a second Ag and dielectric layer..... | 33 |
| 4-12. -1+1S Top Side (Sa=0.74um)..... | 33 |
| 4-13. -1+1S Bottom Side (Sa=0.342um). | 33 |
| 4-14. Ability to produce highly smooth ink films by use of novel lift-off process to obtain self-supported ink films..... | 34 |
| 4-15. Self-supported Rolled Capacitor | 35 |

INTRODUCTION

The increasing demand for miniaturized electronic devices has grown the need for rechargeable micro-power sources. Though lithium and lithium ion batteries have been utilized in these applications since the late 1990s, other energy harvesting technologies such as thermal, mechanical and solar, are now being used.¹ The advantage of using energy harvesting technologies to recharge batteries is that they enable systems to be self-powered. However, the lifetime of any battery is finite, which may be a major problem when placed in a permanent structure, such as a concrete support structure, engine or biomedical implant.² Batteries also cannot provide the peak power for some portable electronic devices without increasing the bulkiness or weight of the device. With developing electronic markets searching for thinner, lighter weight, lower cost and more conformable solutions, printed electronics offers a possible solution to meeting these goals, but a complementary energy source to batteries is still missing.³

Electronic capacitors are used to provide charge storage. Their ability to endure millions of cycles and fast charge/discharge rates enables energy densities to be maintained for the balancing of circuitry in electronic devices.^{4,5} For power or significant energy storage applications, multilayer capacitors or supercapacitors can be used to enhance battery performance, which would help batteries fill current and future energy needs.⁶

The printing of multilayer capacitors offers an inexpensive manufacturing process for producing such devices and the ability to print supercapacitor electrodes, supercapacitors, and batteries are well documented.^{5,6,7,8} However, everything reported to date has involved the printing of various functional inks on rigid or flexible substrates. The type of substrate used is often dictated by the processing temperature requirements of the functional materials printed and flexibility requirements of the end product. This study focused on the fabrication and testing of

self-supporting printed multilayer capacitors. The roughness, flexibility and density of the printed layers were characterized. A completed capacitor consisting of two dielectric ink films sandwiched between a single silver later was printed and tested. The capacitor was also rolled to demonstrate the feasibility of producing a multi-stacked capacitor. The benefits of this research include defining the design and commercial potential for self-supported printed energy storage and advancing the technical knowledge for self-supported printed electronic devices. The findings of this study should also greatly advance work being performed in printed sensors and active transistor devices.

LITERATURE REVIEW

Capacitor and Supercapacitor Technologies

The direct printing of passive (electrodes, resistors, capacitors) and active (thin film transistors, photovoltaics, organic light emitting diodes) devices has gained significant attention as a low cost manufacturing method for flexible electronics. As the global need for energy continues to rise, the risk of facing a supply imbalance also grows. Concerns on how the world will keep pace with growing energy demands have led to increased efforts to find new technologies for harvesting and storing energy. Some of the energy harvesting technologies being explored are light, human movement, vibration and heat, based on technologies such as photovoltaics⁹, electrodynamics¹⁰, and piezoelectronics¹¹.

The harvesting of renewable energy offers just one part of the needed solution. Once harvested, efficient technologies to store the energy are required. Batteries are the most predominant technology used¹², but other technologies such as eutectic systems¹³ or mechanical methods, such a flywheel¹⁴ and hydroelectric storage¹⁵, can be used.

The two most significant criteria for the performance of an electrical energy storage device are power and energy density. Power density is a measure of how fast energy can be transferred per unit mass into a device (J/Kg s). Energy density is the

amount of energy stored per unit mass (J/Kg). Both of these criteria are especially important when device portability is needed.¹⁶

Two major types of energy storage devices are batteries and capacitors. Batteries directly convert chemical energy to electrical energy through the generation of charge from redox reactions that take place at the electrodes of the battery. The generated charge creates a voltage between the battery's cell terminals. The concentration and chemical species within the battery determines the voltage output. In contrast, capacitors store energy by charge separation. A basic capacitor consists of a dielectric electrolyte sandwiched between two parallel electrodes capable of establishing an electrical potential. The dielectric electrolyte can be either an ionic solution or solid material. When a closed circuit between the two electrodes is formed the electrical potential is released generating a power density.¹⁷ The two main functions of a capacitor are to charge or discharge electricity and to block the flow of direct current (DC). The function of charging or discharging energy is used in smoothing the circuits of power supplies and backing-up circuits of microcomputers. The function of blocking DC flow enables them to be used as filters to block undesirable frequencies in a circuit. In general, capacitors do not efficiently utilize the material from which they are fabricated so their energy densities are typically low.¹⁷

Electrolytic capacitors evolved from the basic capacitor design. They are similar to batteries, but have an anode and cathode composed of the same materials. There are aluminum, tantalum and ceramic capacitors.¹⁸

The next evolution in capacitor technology was the creation of electric double layer capacitors, EDLCs, which store electrical charge at a metal/electrolyte interface. The main component of this device is activated carbon, which is used in the electrode construction of these capacitors. This technology served the needs of industry for many years, then experienced resurgence as interests in electrical storage technology for medical devices, miniature electronic devices and applications requiring very short high power pulsed devices. EDLCs complement batteries by supplying a high power density and low energy density when needed, while lasting longer than batteries. In comparison to conventional capacitors, they have higher energy

densities. The disadvantage to EDLCs is that they suffer from low energy density. To address these problems, researchers have explored mixing transition metal oxides with the activated carbon used as the electrode material. This mixing enhanced the specific capacitance by a factor of 10-100, depending on the type of metal oxide used.¹⁹ The increased performance brought about by this technology introduced a new class of capacitors called supercapacitors or pseudocapacitors.

Capacitors with very high energy densities are referred to as ultracapacitors or supercapacitors.¹⁹ Supercapacitors have been the focus of much research over the past 10 years.²⁰ The superior performance in these devices in comparison to capacitors is shown in Figure 2-1.

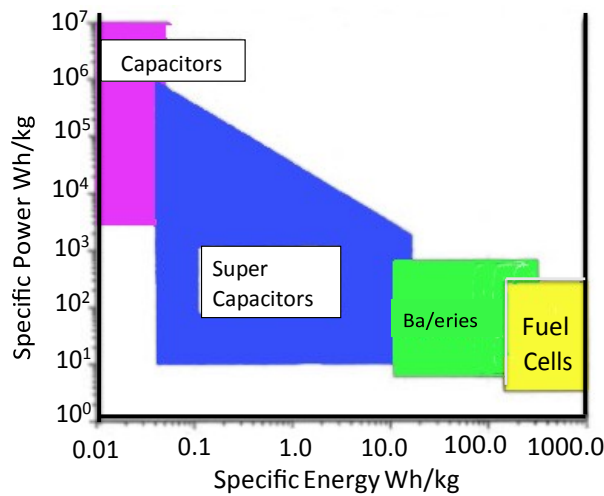


Figure 2-1. Comparison of different storage devices (Modified From Winter and Brodd²¹)

As shown in Figure 2-1, the difference between a supercapacitor and capacitor is the specific power over the specific energy rate of each device.

The general equations for capacitance (1) and energy storage (2) were first proposed by Helmholtz in 1853.²²

$$C = (A\varepsilon_1\varepsilon)/d \quad (1)$$

$$E = \frac{1}{2}(CV^2) \quad (2)$$

Where,

C is capacitance (Farads),

E is the energy stored (joules or watt-sec),

ϵ_0 is the permittivity of free space, equaling 8.8541×10^{-12} F/m,

ϵ is the relative permittivity of the dielectric layer, or dielectric constant,

A is the total surface area of the electrodes (m^2),

d is the distance between the two parallel electrodes (m),

V is the established potential between the electrodes (volts).

From equation 1, it is clear that to achieve very high supercapacitor performance, a combination of maximizing the plate area, minimizing the distance between plates and selecting a dielectric material to maximize the effective permittivity is needed. For printed capacitors, the distance between plates is limited by the thickness of the printed dielectric layer, which is often determined by the printing method used. The permittivity is based on the properties of the dielectric material, which can be deposited/printed, or the original substrate itself. Using a number of geometric techniques; such as, stacking alternating plates or rolling up a flat, flexible capacitor can effectively manipulate the area.²³

By combining these two equations, the peak energy density per unit mass can be written as:

$$\text{Energy Density} = E\rho = (\epsilon_0/2) (A/d)(\epsilon V^2/\rho) \quad (3)$$

Where ρ is the device density per unit mass and V_b is the breakdown voltage of the dielectric material. V_b is used instead of V in order to allow the properties of different dielectric materials to be compared.

A close examination of (3) shows three parts: a constant term ($\epsilon_0/2$), a geometrical term (A/d) and a materials property term ($\epsilon V_b^2/\rho$). Hence, the energy density of a capacitor can be achieved by altering the geometry and properties of the materials used.²⁴

The most sophisticated types of ultracapacitors are electrochemical capacitors, ECCs, and electric/electrochemical double layer capacitors, EDLCs. Both devices have capacitance values that are orders of magnitude higher than traditional capacitors, hence the term super and ultra. An ECC consists of two electrodes immersed in an ionic solution, which enables the accumulation of charge at the double layer interface. The most common uses of ECCs are in hybrid electrical vehicles and in solar and wind power facilities where they are used to supply intermittent energy. EDLCs store charge from ions supplied from an electrolytic solution on high surface area electrodes typically made from activated carbon. These unique properties enable them to fill the gap between batteries and conventional capacitors. Both ECC and EDLC technologies are commercially available. The main use of EDLCs are in applications where energy conservation, electrical power load leveling, and high power millisecond long pulse delivery is needed, for example to start an engine or automotive braking systems.²⁵

The basic differences between the design and construction of ultracapacitors are shown in Figure 2-2.

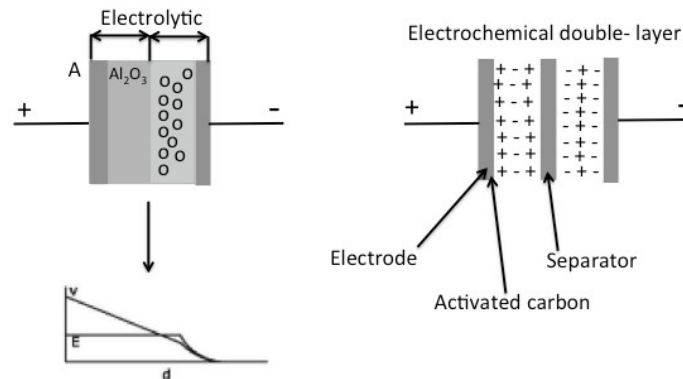


Figure 2-2. Schematic presentation of electrolytic capacitor and electrical double layer capacitor
25
 (Recreated from Jayalakshimi, 2008)

Two other types of capacitors are ceramic and film capacitors. Ceramic capacitors are constructed from alternating layers of metal and ceramic, with the ceramic serving as the dielectric. Multilayer ceramic capacitors (MLCs) typically contain around 100 alternating layers encased in two ceramic layers. They are

fabricated by screen-printing both the conductive metal and dielectric layers and co-sintering them together. The most commonly used material for the electrode and dielectric layers is Ag-Pd and BaTiO₃, respectively^{23,24}.

Since the year 2000, when the communications market began to flourish, the demand for MLCs has increased to keep pace. Other ceramic materials that have been identified are CaZrO₃, MgTiO₃, and SrTiO₃. Mn and Ca are some of the other electrode materials being used. Film capacitors, just as the name suggests, are made using thin films of polyester or polypropylene as the dielectric and meta-glazed capacitors, which consist of Al electrodes created by the vapor deposition of Al onto a polyester, polypropylene, or polycarbonate film.^{26,27}

Recent printed electronics research has examined nano gold, graphene, nano silver, nano copper, single-wall and multi-wall carbon nanotubes (CNT) as electrode materials.^{8,23,27,28,29,30} A comparison of different conductive inks for use in printed electronics is shown in Table 2-1.

Table 2-1. Comparison of Conductive Inks for PE Applications²⁸

| Ink | Conductivity | Oxide | Curing | Substrate use | Film cohesion | Process limitations |
|----------------|---------------------|-----------------------|-------------------|----------------------|----------------------|----------------------------|
| Silver | Excellent | Conductive | High temp. | Limited | Good | |
| Carbon | Average | Does not form | Low temp. | | Poor | |
| Copper | Good | Non-conductive | High temp. | Limited | Good | |
| Polymer | Average | Does not form | Low temp. | | | Low solubility |
| CNT | Excellent | Does not form | Low temp. | | | Toxic |

In addition to the conductive inks listed above, graphene has also been heavily studied as a conductive material for pseudocapacitors. Graphene is a non-toxic nano-material, which is readily dispersible; it is the most conductive form of carbon. It does not require high temperature sintering and therefore can be used with plastic film and paper substrates. It also gives the ability to be deposited as very thin layers, and is less expensive than silver, copper, and CNT inks. A comprehensive review of recent research performed using graphene in energy harvesting/storage devices and printed

electronics was recently performed by Grande et al.⁸ Nair et al.³¹ showed graphene to be a feasible alternative for indium tin oxide (ITO) in OPVs, due to the ability of a single layer of graphene to transmit 98% of total incident light. Blake et al.³² reported films of graphene having a sheet resistivity of approximately 6 k Ω /sq. This corresponds to a bulk resistivity of about 2×10^{-6} Ω -m. The sheet resistance of graphene was found to depend on the quality of the graphene sheets. The fewer the defects in the sheets, the lower the sheet resistance. Several reports have also shown the method of synthesis to greatly impact the sheet resistance of graphene.

The use of graphene to produce supercapacitors with specific energy densities comparable to Ni metal hydride batteries for hybrid vehicles was recently demonstrated by Liu et al.³³ The supercapacitors produced have the advantage of being rechargeable in less than 2 minutes, which is faster than what can be obtained with current hybrid battery technologies. Wang et al.³⁴ and Yu et al.³⁵ synthesized 25 nm thick graphene/graphite sheets using a vacuum filtration method, which enabled a capacitance of 135 F/g to be realized. The graphene sheets produced by this method were found to be flexible and transparent, thus capable of being used in applications where transparent supercapacitors would be needed.

The use of hybrid CNT/graphene composites in polyethyleneimine (PEI) and polyaniline (PANI) in supercapacitors was explored by Yu & Dai³⁶ and Wu et al.³⁷, respectively. Capacitances of 120 F/g and 210 F/g, respectively, at a current density of 0.3A/g were achieved. Han et al.³⁸ used polypyrrole (PPy) and obtained a capacitance of 223 F/g at a current density of 0.5A/g. PPy has the advantage of being more stable under ambient conditions in comparison to PANI.

Jari et al.³⁹ explored the use of graphene to create supercapacitors. In their work, supercapacitor electrodes of 2 cm² and 0.5 cm² using activated carbon were prepared. They showed the standard 2 cm² capacitors to have typical capacitance values of 30-35 F/g with only the activated carbon mass taken into account. They also compared electrodes printed from 3 commercial silver inks to graphene electrodes and found no practical differences in their conductivity values with typical sheet resistances of 0.03-0.05 Ω /□ for 20-30 μ m thick layers.³⁹

Graphene oxide, GO, has also been studied. Although alone it is non-electrically conductive, the addition of thermal, chemical, and photothermal processes reduces it to graphene. A recent study by Le⁴⁰ showed the ability to inkjet print a 0.2 wt% water based GO ink with a viscosity of 1.06 mPa.s and surface tension of 68 mN/m on a Dimatix inkjet printer. Once printed, GO electrodes were thermally reduced under N₂ atmosphere at 200°C to graphene. Though these ink characteristics were outside the recommended ranges for normal inkjet printing (e.g., 10-12 mPa.s and 28-32 mN/m), Le found that by manipulating the firing voltages of the nozzles as a function of time spherical ink droplets without clogging could be produced. A spatial resolution of ~ 50 μm was achieved. Titanium foils from Sigma Aldrich (100 micrometers thick, 99.99% purity) were used as a comparison for electrochemical performance. The use of two identical electrodes clamped with a Celgard separator produced a specific capacitance of 48-132 F/g in the scan range of 0.5 to 0.01 V/s for the graphene electrodes and 96.8% of the capacitance was retained over 1000 cycles. It was also shown that graphene electrodes prepared by conventional powder based methods were similar in performance to the inkjet printed electrodes.³⁷

Although graphene and carbon nanotube inks are good alternative electrode materials to silver, the printing of these nano-materials can be difficult due to their hydrophobic nature, which causes them to segregate in water unless surfactants are added, or their surfaces functionalized.⁴⁰ Silver inks, on the other hand, are well established in the market place. Inkjet, screen, flexo, and gravure Ag inks are readily available and have been used as electrode materials in many PE applications. Solvent based silver inks are of special interest to this study, due to their high water resistance, which is needed to allow for the lifting off the printed layer through the use of a sacrificial water-soluble base layer.

Printed supercapacitors need to be flexible and capable of being printed or attached onto multiple substrates. To be useful, the performance of the storage device should meet the life expectancy of the product. Low cost and ease of production would increase their acceptance. Printed energy sources that could be integrated into

a printed device in-line would greatly reduce the fixed production costs of supercapacitor systems.

This study focused on the feasibility of screen-printing a self-supported capacitor. The capacitor was fabricated using a commercially available solvent-based silver ink and UV dielectric ink. The novelty of this work was that a newly discovered lift-off process was used for the first time to obtain a self-supported capacitor. It was demonstrated that the self-supported printed capacitor could be rolled, resulting in multi-stacked silver and dielectric layers. The findings suggest that it may be possible to create a supercapacitor by rolling a self-supported dielectric-silver-dielectric-silver printed stack.

Lift-Off Processes

Several methods for the lift-off of printed electronic devices have been reported.^{41,42,43,44} Ogier et al.⁴¹ describe the use of a lift-off ink to enable the printing and lift-off of organic electronic devices, mainly organic light emitting displays, OLEDs. The lift-off ink is printed as a negative image then sequential device layers are printed on top. To lift-off the device, a lift-off solution, which dissolves the lift-off ink, but not the device layers, is applied. The process requires the use of ultrasonic agitation, stirring, a spray liquid medium and/or heat to be used. Broer et al.⁴³ describe a laser lift-off process that uses the wet casting of a plastic coating, containing a UV absorbing additive, to a substrate followed by the screen or inkjet printing of thin film electronic elements to fabricate an active display matrix. The laser is used to lift-off the plastic layer after it has been printed from the carrier substrate. Greer and Howard⁴² describe a lift-off process to remove any unwanted areas from a metallization layer to form a layer of masking material over a semiconductor device. Lift-off occurs upon heating of the device to a temperature where the metal melts on the masking layer and forms globules when it cools, which can be removed. Rogers et al.⁴⁴ described a carrier layer coated with a sacrificial layer to which a stretchable substrate is attached. The stretchable substrate is printed with

electronic devices, and removed to produce a self-supporting stretchable device. This process can presumably make strain independent electronic devices.⁴⁴

Overview of Printing

Printing is an attractive process for the manufacture of multilayer capacitors due to its low cost and low waste in comparison to traditional photolithography. Unlike photolithography, printing is an additive process that can be performed at high speeds. Printing also allows the direct printing of multilayer capacitors onto products that it might power (such as a mobile phones and consumer packages).

The four major printing processes being utilized to pattern functional ink layers are the flexographic, rotogravure, inkjet and screen-printing processes. The process and ink requirements for each are different. The differences in ink properties requirements for each process are shown in Figure 2-3. As shown in Figure 2-3, the ink viscosity requirements for the screen-printing process are at the highest of any of the processes. The high viscosity of the screen-printing inks is required due to the deposition process, and the need for the inks to hold specific drying and leveling properties. The high viscosity characteristic of the screen-printing ink also gives the screen-printing process the ability to print highly thick layers in comparison to the inkjet and gravure processes, as can be seen in Figure 2-4. The ink film thickness and feature sizes attainable for each process are shown in Figure 2-4. Figure 2-4 shows the vast differences between the processes and achievable ink film thicknesses. From the figure, it is seen that the screen-printing process produces the highest ink film thicknesses of all the processes.

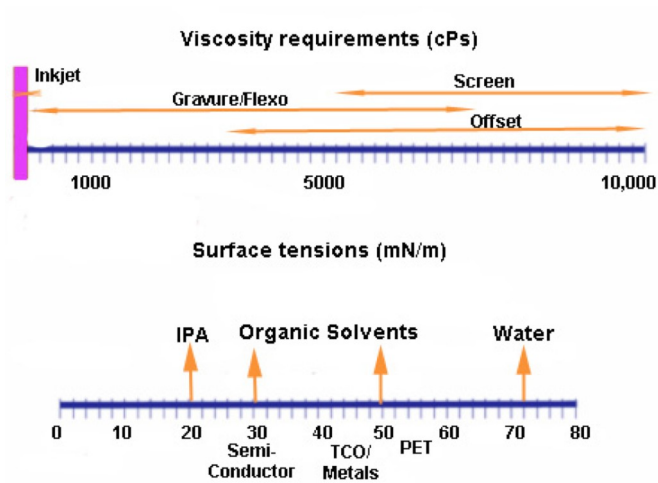


Figure 2-3. Comparison of Ink Properties ⁴⁵

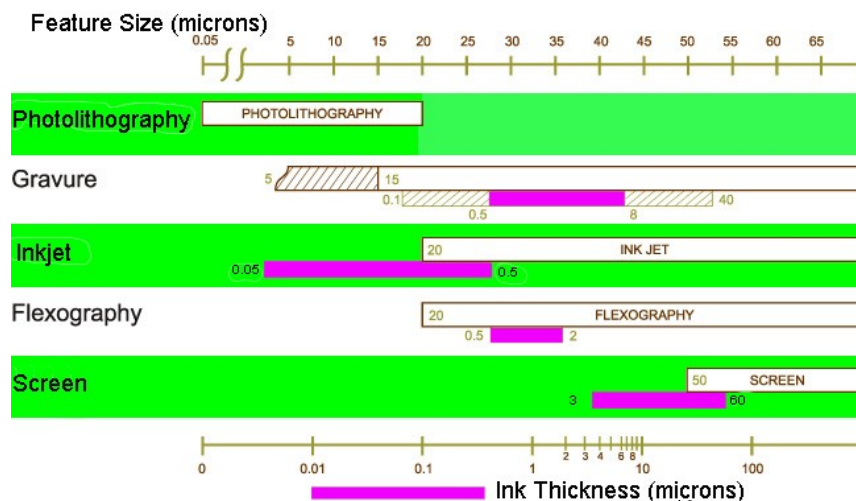


Figure 2-4. Comparison of Ink Film Thicknesses ⁴⁶

Since this study only involves the screen-printing of functional materials, only this printing process will now be reviewed.

Screen-Printing

Screen-printing is a stencil process wherein a stencil is applied to a mesh held in tension over a rigid rectangular frame. Highly viscous ink is pushed through the open area of the stencil, with a resilient squeegee, where it contacts the substrate to be printed.⁴⁷ A schematic of the process is shown in Figure 2-5. The advantage of this

printing process is that thick ink films and fine lines can be printed. The screens, depending on the materials used, are also resistant to many solvents. Large and small particle inks can be printed and many functional material ink types are commercially available. Screen-printing can also be performed on rigid or flexible substrates. Sheetfed presses are common, as well as rotary screen presses for the higher throughput roll-to-roll printing of materials.

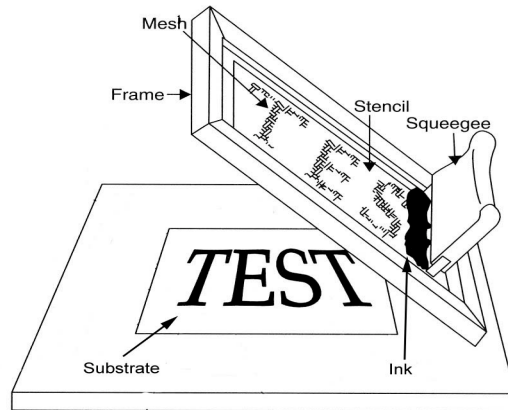


Figure 2-5. Schematic of Screen-printing Process (Modified from Ingram⁴⁷, p. 2)

Regardless of the screen-printing press used, sheetfed or rotary screen, the image carrier will consist of the following components: the frame, the woven screen, and the stencil. The frame is the support mechanism for the tensioned fabric. The two combined make-up the screen. Frames can be made from wood or metal. Wood frames can be easily constructed to inexpensively provide a broad range of sizes. They are moderately durable and easily sealed with a varnish to provide moisture resistance. However, in comparison to metal frames, they distort more, especially at higher tension levels, making them more difficult to register. Metal frames are typically made of aluminum or steel. Lightweight aluminum frames are easier to handle than steel frames. Metal frames are impervious to most ink solvents and cleaning fluids. They are hollow and available in different wall thicknesses, which impacts strength.⁴⁸

The woven screen fabric is attached to the frame under tension. Adhesives are used with metal frames to attach the fabric, while staples or cords are used with

wooden frames. If cords are used, a groove must be cut into the wooden frame so that the cord can be driven into the groove once the fabric is positioned. The woven screen-printing fabric serves the functions of supporting the stencil and holding or metering the ink through the open areas. The mesh or thread count (how many threads per inch are present) plays a dominant role in ink metering. The mesh count determines the distance between the threads or the mesh opening area. The larger the open area between threads, the more ink deposited during printing. Another important characteristic of the screen is the emulsion thickness. The emulsion thickness also plays a key role in the achievable ink film thickness. The thicker the emulsion, the thicker the ink film will be. The masking of the screen by the emulsion is shown in Figure 2-6, where the covered (non-image) and open (imaged) areas of a screen are shown. In the far right image of Figure 2-6, it is apparent how the thickness of the emulsion directly affects the achievable ink film thickness. Examples of different weaves and mesh sizes are listed in Table 2-2. Table 2-2 also shows differences between the mesh size openings, mesh diameters, and mesh thicknesses. A comparison of the listed values demonstrates the relationship these variables have on one another. For example it may be seen that, as the mesh count decreases, the percent open area increases. The larger the particles in an ink, the greater the open area needed to allow the particles to pass through the screen without binding (clogging). Therefore, there is a need to increase the wire diameter, and mesh thickness to increase the percent open area. Increasing the open area and enables thicker ink films to be printed, at the expense of print resolution. It is therefore a requirement to fully understand the needs of a specific print job prior to optimizing the screen specifications for any particular job.

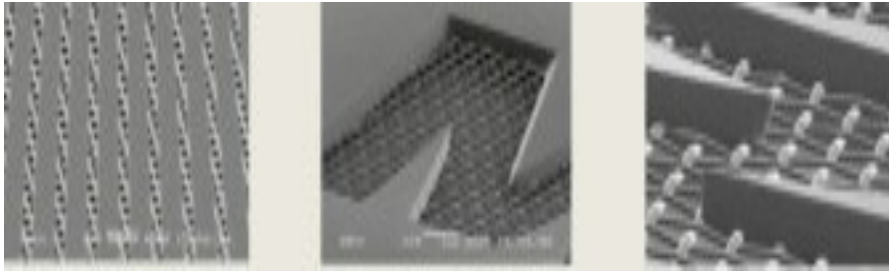


Figure 2-6. Pictures of open and masked areas on a screen and magnified view of the emulsion layer to show the thickness of this layer

| Table 2-2. Mesh Specifications ⁴⁹ | | | | |
|-----------------------------------------------|-------------|------------------------------|-----------------------------|-------------------------|
| Stainless Steel Mesh - Standard Wire Diameter | | | | |
| Mesh Count | % Open Area | Wire Diameter (inches)=0.001 | Mesh Opening (inches)=0.001 | Mesh Thickness (inches) |
| 60 | 50.0 | 0.0045 | 0.0122 | 0.0090-0.0088 |
| 80 | 49.5 | 0.0037 | 0.0088 | 0.0080-0.0088 |
| 105 | 46.9 | 0.0030 | 0.0066 | 0.0061-0.0067 |
| 120 | 47.3 | 0.0026 | 0.0057 | 0.0063-0.0068 |
| 145 | 46.4 | 0.0022 | 0.0047 | 0.0045-0.0049 |
| 165 | 44.9 | 0.0020 | 0.0042 | 0.0041-0.0045 |
| 180 | 45.7 | 0.0018 | 0.0038 | .0039-.0043 |
| 200 | 46.2 | 0.0016 | 0.0034 | 0.0033-0.0038 |
| 200 | 33.6 | 0.0021 | 0.0029 | 0.0041-0.0046 |
| 220 | 45.9 | 0.0014 | 0.0029 | 0.0030-0.0033 |
| 250 | 36.0 | 0.0016 | 0.0024 | 0.0033-0.0037 |
| 270 | 38.7 | 0.0014 | 0.0022 | 0.0029-0.0034 |

| | | | | |
|------------|-------------|---------------|---------------|----------------------|
| 290 | 44.1 | 0.0012 | 0.0024 | 0.0025-0.0028 |
| 325 | 41.3 | 0.0011 | 0.0020 | 0.0023-0.0026 |
| 400 | 36.0 | 0.001 | 0.0015 | 0.0019-0.0023 |

The selection of the screen fabric is extremely important. Some general rules of thumb to use when selecting a screen fabric are⁵⁰:

- Monofilament fabrics are more abrasion resistant. They generally clean easier and pass ink more readily than multifilament fabrics. They are available in finer mesh counts than other types of fabrics.
- Multifilament fabrics are thicker, rougher than monofilament fabrics and are typically used to deposit thicker ink films.
- The mesh opening should be at least three times larger than the average particle size within an ink to reduce the tendency for screen binding (plugging of screen openings).
- The thinner the thread, the thinner the deposited ink film.
- The finer the features to be printed, the finer the mesh should be.

In addition to opening size, the resistance of the mesh material to solvents and additives in the ink is also important along with costs. Some common screen fabric materials used for the printing of functional inks are stainless steel, monofilament nylon and polyester and nickel-plated polyester.⁴⁹

The stencil blocks the screen fabric from allowing the ink to reach the substrate, therefore determining the non-image area of the screen. The selection of the stencil material depends on the print requirements, the type of mesh and ink to be used, and the length of the print run. The majority of stencils used for printed electronic applications are produced directly, whereby a light sensitive emulsion is applied to the screen, dried, then exposed to a light source that hardens the emulsion in the non-image areas of the screen. The non-hardened or imaged areas are then washed away. The resistance of the emulsion must be matched to the ink used⁴⁹.

The squeegee runs across the screen and pushes the ink through the open areas of the mesh (where the stencil has been washed out) and on to the substrate beneath the screen. There are varieties of squeegee materials that can be used. The three most important characteristics of a squeegee are its solvent resistance, hardness and shape. The material used to make the squeegee determines its hardness and solvent resistance. Polyurethane and rubber are common materials used. Polyurethane squeegees are more solvent resistant, but more expensive. The hardness of the squeegee can be described as hard, medium and soft. A hard squeegee is most commonly used to print on glass, where spreading is difficult to control due to glass being non-porous. Medium hardness squeegees are used to print on most materials because by varying the pressure applied, the amount of spreading on a porous substrate can be altered. Soft squeegees are typically used when printing is done by hand. This is because a soft squeegee will flex more, allowing the operator to have more control over the amount of pressure applied. The thickness of the ink deposit is determined by the angle of squeegee. Thicker ink films are deposited at lower squeegee angles.

Problem Statement

The printing of electronic devices on flexible and rigid substrates is well known, but having the devices supported by a substrate is not always advantageous. This is especially true for cases where the rigidity of the substrate limits the extent to which the device can be bent or rolled, or where the substrate compatibility issues to the surface to which it is to be attached is faced. The ability to bend or roll devices can improve the attachment to surfaces; enable its placement in confined spaces and advance efforts to further miniaturize devices. In this research, a sacrificial water-soluble polymer layer was used to produce self-supported (substrate free) printed conductive and dielectric ink films of different thicknesses, as well as a completed capacitor. The electrical and mechanical properties of these films and the capacitor

were measured. Such measurements have not yet been reported and should therefore advance our understanding of their properties at different thicknesses.

EXPERIMENTAL METHODS

Creation of Sacrificial Layer

A sacrificial water-soluble alginate coating was applied on Melinex ST 506 PET (DuPont, Chester, VA). The alginate (S-160-QD, SNP Inc., Durham NC) was applied to the PET as a 6% aqueous solution using a #14 and #20 Meyer rod. By using different Meyer rods, films of different thicknesses were obtained. The alginate solutions were prepared by slowly sprinkling the appropriate amount of dried alginate into a pre-weighed amount of deionized water under agitation. Once all alginate was added, the solution was allowed to mix for 60 minutes to assure complete hydration. The solution was then placed in a closed container in a refrigerator overnight to enable it to degas. After 24 hours, the solution was removed and brought to room temperature, approximately 70°F, before applying it to the PET films, which were cleaned with isopropyl alcohol just prior to application of the alginate solution. After coating, the samples were placed in a TAPPI standard test room held at 50% RH and 73.4 °F (allowing for reproducible and consistent drying conditions). After the initial roughness measurements were conducted, it was apparent the amount of particulate matter in the air throughout the building and in the TAPPI room were significant, so measures were taken to keep the coated samples in an enclosed (“clean”) environment during drying. The samples were placed in a Carron RH chamber at approximately 70°F for 24 hours, then removed and kept in a covered plastic container immediately prior to and just after printing and drying/curing.

Design of Experiments

After characterizing the properties of the alginate films, single and multilayer prints were prepared according to the DOE shown in Figure 3-1. The DOE is a combination of 2 DOEs. The first one contains only the alginate (+1 and -1 conditions) and single layer prints, while the second one contains the multilayer prints. The design was created in this way to allow for the characterization of the alginate films and single layer prints alone, before characterizing the multilayer prints. By characterizing the alginate and ink films in this way, the impact of each on the final device will be better understood. The print pattern used for this portion of the study is shown in Figures 3-2 and 3-3. Figure 3-2 shows each individual layer and how they were overlaid onto one another, while Figure 3-3 depicts the completed final device. The thickness, roughness and electrical properties of all printed samples were measured to determine the influence of ink type, film thickness, and ink density on the mechanical and electrical properties of the ink films.

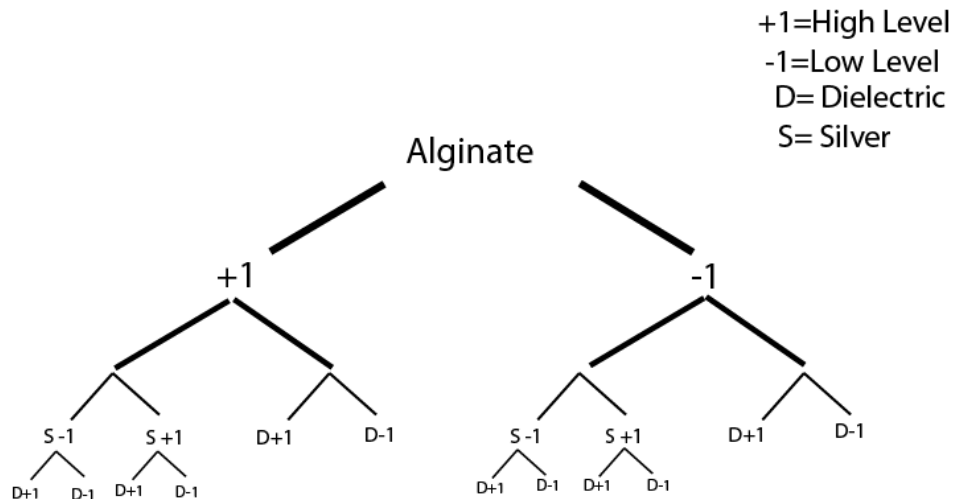


Figure 3-1. Experimental Design (-)1 for alginate obtained using a #14 Meyer rod, and (+)1 obtained using a #20 Meyer rod). S-1 and D-1 refer to single layer silver and dielectric, and S+1 and D+1 refer to double layer silver and dielectric respectively

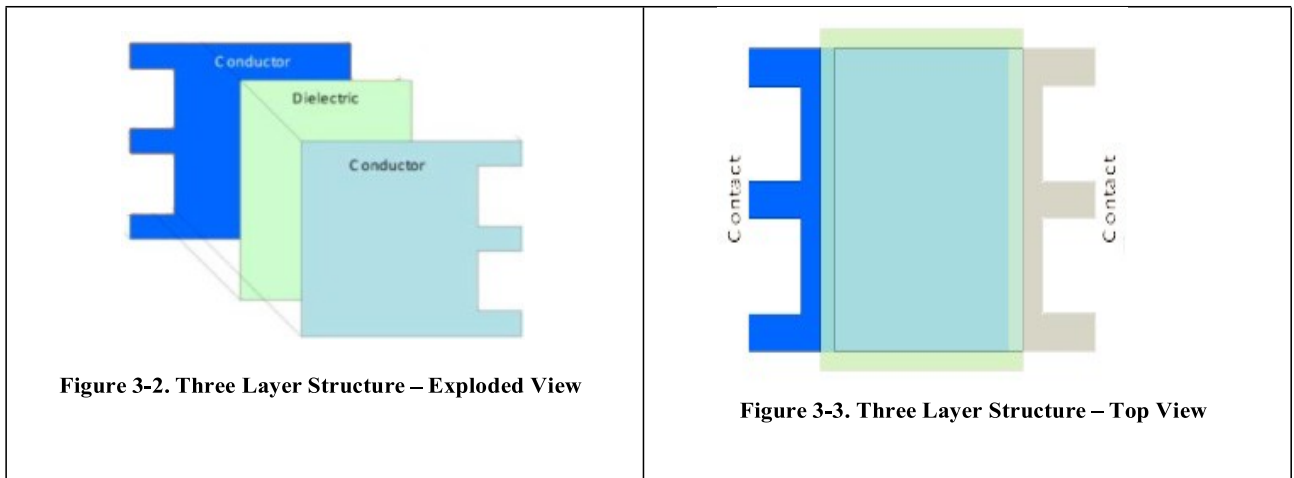


Figure 3-2. Three Layer Structure – Exploded View

Figure 3-3. Three Layer Structure – Top View

Preparation of the Alginate Films

While preparing the alginate films of different thickness from the 6% solution, it was observed that the PET films were curling upon drying and the alginate film layers were cracking. To alleviate this problem, glycerol was added to the solution of alginate to help plasticize the film. After observing that the glycerol helped to prevent both issues, a study was carried out to determine the best level of glycerol addition to obtain good film strength, and flexibility after drying.

Multiple experiments were performed varying the amounts of glycerol added. The addition level that was found to give the most uniform alginate film was 20% glycerol on weight of dry alginate. At addition levels higher than 20% the films were tacky to the touch. Films prepared using # 0.5, 1.0, 6.0, 8.0 and 10 mil Byrd applicators were very thin and could not be easily removed and handled. However, films prepared using #14 and 20 Meyer rods were thick enough to be easily removed and handled. The thicknesses of these films were found to be 6.88 and 14.41 microns, respectively. In addition to creating alginate layers with the #14 and #20 rods, it was observed that much thicker alginate films of approximately 300-400 microns formed very tough films, however, due to their higher thickness, they did not dissolve as readily in water so the time required to dissolve the films was much longer, which

was not desirable. For this reason, all films were prepared using the #14 and #20 Meyer rods.

Printing

After drying, the roughness (S_a) and thickness of the alginate films were measured with a Bruker GT-K Interferometer microscope. Single and double layers of the silver, and dielectric inks, listed in Table 3-1, were screen-printed onto the alginate coated PET samples using an AMI MSP-485 semi-automated screen printer. Double layer samples were accomplished by first printing and drying/curing the first layer prior to printing the second layer on top of the first. The samples were then cured/dried using a Fusion UV drier equipped with a D bulb⁵¹. The samples were passed through the Fusion UV drier at a 16 speed, until fully cured (no longer tacky to the touch), which took anywhere from 3-4 passes. Using an IR temperature probe, the dryer temperature within the Fusion UV drier was measured to be 130 degrees F, which was sufficient to fully dry the silver ink after 3-4 passes. The pattern printed for each ink was a 5×5 cm solid block. The specifications for the screen used are given in Table 3-2. The screen specifications were produced with aid from the above table (Table 2-2 “Mesh Specifications”) with the desire to produce an approximately 10-micron thick dry ink film.

Table 3-1. Commercial Inks Used

| Supplier | Ink Type | Commercial Name |
|--------------|----------------------|--------------------|
| Sun Chemical | Thermal Flake silver | AST 6200 |
| Henkel | UV dielectric | Electrodag PF-455B |

Table 3-2. Screen Specifications

| Manufacturer | Specifications |
|------------------------------|----------------------------------------------------------------------------------|
| Microscreen (South Bend, IN) | 230 LPI mesh 0.0011" wire diameter at 45 ° wire angle 10 μm thick emulsion |

Removal of the Sacrificial Layer

After, measuring all the desired properties on the PET printed samples, the samples were wetted with room temperature (71°F) distilled water to dissolve the sacrificial layer of sodium alginate and the printed layers lifted-off the PET. After retrieving the self-supported films from the water, the films were blotted dry and retained for further measurement.

Analytical

After drying the alginate films prepared using the #14 and 20 Meyer rods, the roughness (S_a) and thickness of the films were measured with a Bruker GT-K Interferometer microscope, as well as the contact angles and surface energies. The thickness and roughness of the printed films were also measured using the Bruker GT-K Interferometer in addition to the electrical and mechanical properties.

The surface energies were determined by Owens-Wendt method, by measuring the contact angles of two liquids of known surface tension (water and methylene iodide) with a First Ten Angstrom dynamic contact angle measurement device.^{52,53} The resistance of the silver ink layers and capacitance of dielectric ink layers were measured with the instruments listed in Table 3-3. The dielectric constant of the dielectric layers were then calculated from the capacitance measurements. The weights and calipers of the free films were then measured and their densities calculated. Attempts to determine the stiffness of the films with a Gurley Stiffness test instrument failed due to stiffness of the films being below the detectable limits of the instrument. Attempts to measure the electrical properties under flexion on a Mark-10 instrument while attached to a Keithley 2602 Dual Source Meter also failed, due to the inability of the sample to survive the test without tearing.

Table 3-3. Testing Equipment and Measurement Parameters

| Test Equipment | Measurement Parameters |
|-------------------------------------------------------------------------------|--------------------------------------------------------------------------------|
| Keithley 4200-SCS Semiconductor Characterization System | Capacitance (for final device only), Resistance, Effective Dielectric Constant |
| Keithley 2602 Dual Source Meter | 1 Ohm to 1 MOhm Surface Resistance |
| Keithley 6517A High Impedance Test Set and ASTM D257 Resistivity Test Fixture | > 1 MOhm Surface Resistance |
| Agilent 4338B Milliohm Meter | < 1 Ohm Surface and Bulk Resistance |
| Agilent E4980A LCR Meter | Capacitance (for final device only), Effective Dielectric Constant |

RESULTS

The surface energies of the alginate coated PET films are shown in Table 4-1. As shown, the surface energy increased with increasing film thickness. This could be because at the higher alginate film thickness, the lower surface energy PET did not influence the measurement, but for the thinner alginate film, it did. This is reasonable explanation when one considers the high solubility of alginate in water. It should be noted that observations were made after running the test that less of the thinner alginate film remained in the area in which the water made contact than for the thicker alginate film (testing took approximately 30 seconds).

Table 4-1. Influence of alginate film thickness on surface energy

| <u>Test Statistic</u> | <u>PET</u> | <u>14.41 microns</u> | <u>6.88 microns</u> |
|------------------------------|-------------------|-----------------------------|----------------------------|
| Polar: [mN/m] | 2.3 | 30.3 | 15.5 |
| Dispersive: [mN/m] | 41.8 | 29.7 | 31.3 |
| Surface Energy:[mN/m] | 43.8 | 60.0 | 46.5 |

The high surface energy of the alginate film is due to the large number of carboxyl and hydroxyl groups in the polymer (See Figure 4-1)⁵⁴. The polar groups attract the polar components of the test fluid (i.e. water H₂O), pulling the fluid's molecules away from one another and toward those contained on the substrate

causing the fluid to spread. This increased spreading then lowers the contact angle at which the fluid contacts the substrate's surface decreasing the fluid's thickness (e.g. water, ink, etc.). The contact angle values used to determine the surface energies are shown in Figure 4-2. It is obvious by the contact angles of both fluids being less than 90 degrees that both fluids wetted the alginate films.

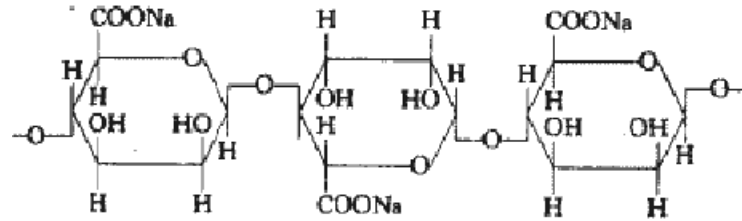


Figure 4-1. Molecular Structure of Sodium Alginate

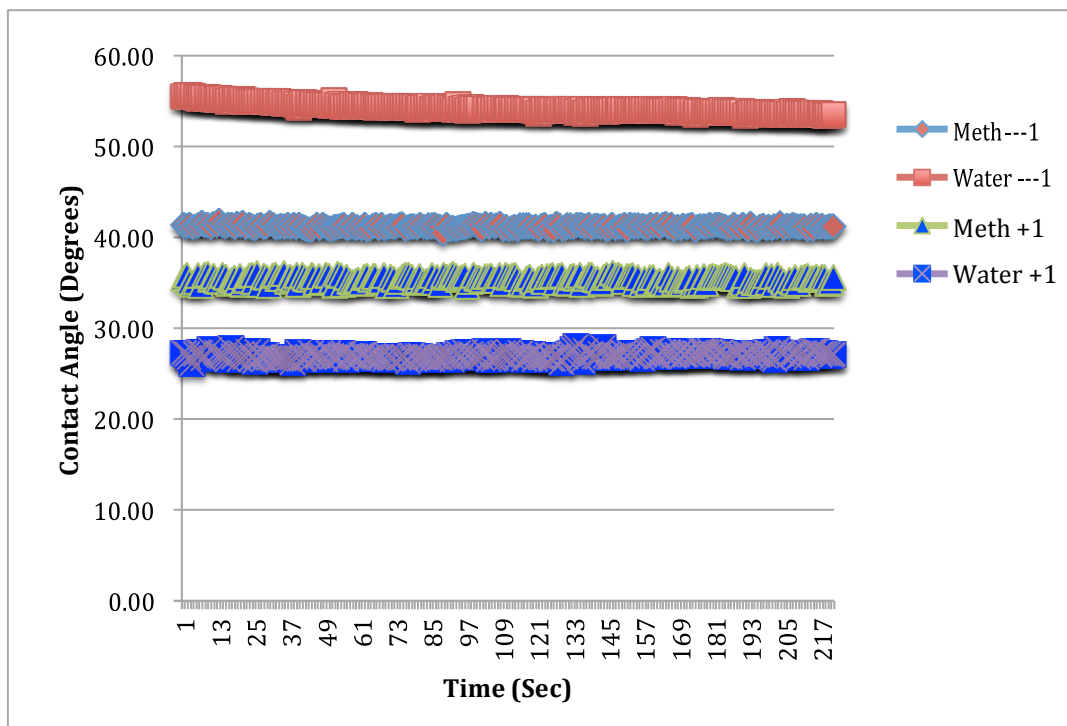


Figure 4-2. Dynamic Contact Angle Measurements of Alginate Films

The roughness values of the 14.41 and 6.88 μm thick alginate films are compared in Figures 4-3 and 4-4. The average roughness, R_a , of the 14.41 and 6.88 μm films are 0.44 and 0.28 μm , respectively. The higher roughness of the thicker

alginate film could be the result of the coarser grooves on the #20 Meyer rod or greater film shrinkage.

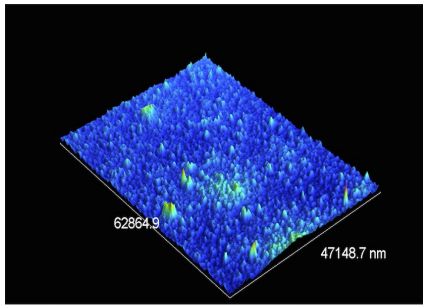


Figure 4-3. Surface roughness of the 14.41 micron alginate film

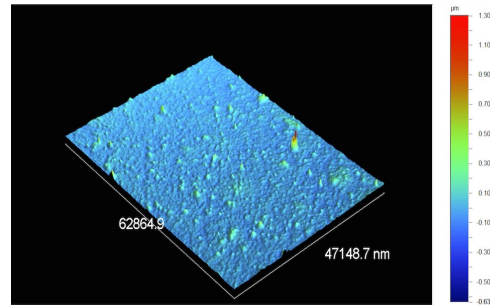


Figure 4-4. Surface roughness of the 6.88 micron alginate film

After fully characterizing the alginate layers, the roughness and thickness of the dielectric and silver layers printed over the alginate films, according to the DOE, were measured. The results are shown in Figures 4-5 and 4-6.

Comparison of Average Alginate and Ink Film Roughnesses

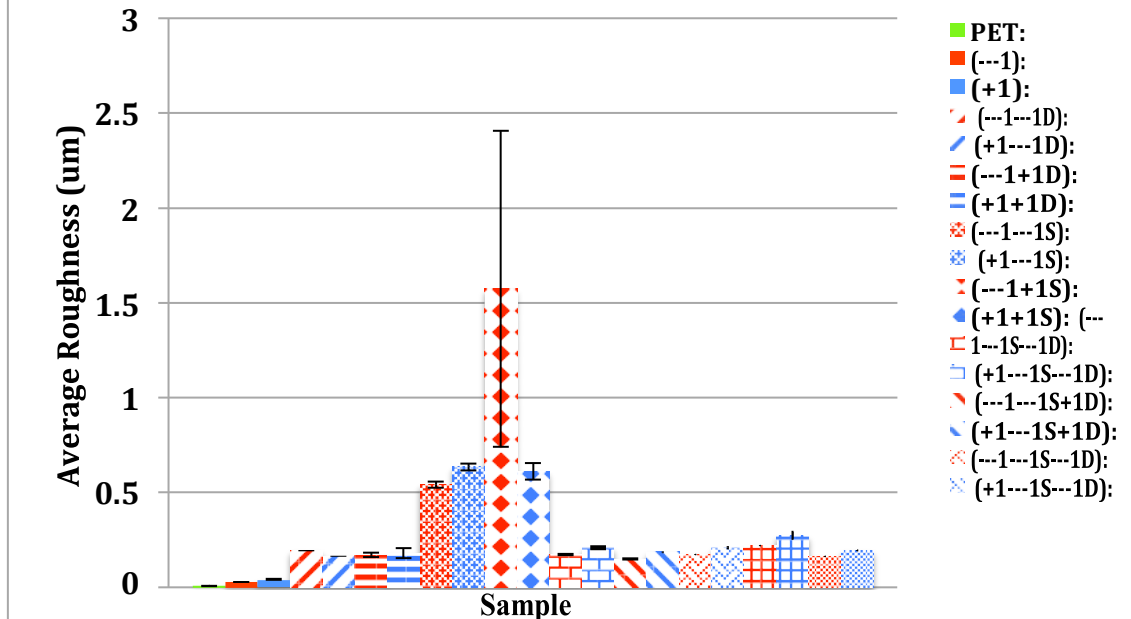


Figure 4-5. Variations in alginate and ink film roughness with printed and coated layers

The roughness values of the silver layers were significantly higher than the dielectric layers due to the presence of silver flakes in this ink. The roughness of the alginate layers had little or no effect on the roughness of either the silver or dielectric layers. This would indicate that the roughness of these layers, as a result of the properties of the ink, screen-printing or drying processes, was great enough to overcome the roughness of the alginate film. Since the roughness of the alginate film was related to its thickness, it can be concluded that the thickness of the alginate film also had no influence on the roughness of the printed layers.

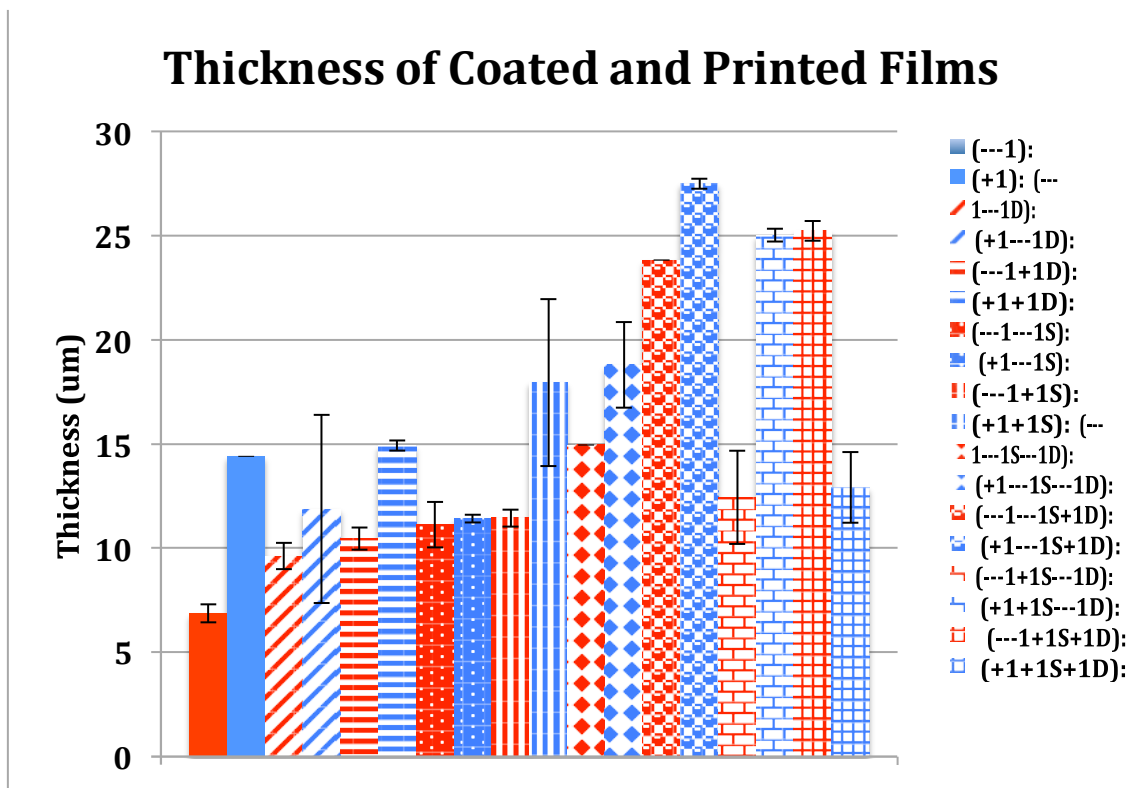


Figure 4-6. Comparison of Film Thickness Values

A comparison of the 14.41 and 6.88 μm alginate printed samples shows an influence of these layers on ink film thickness of both the single and double layer printed silver and dielectric ink films. All dielectric ink films (single and double) were thinner than the silver ink films. It is also seen that all ink films printed on the 6.88 μm alginate films are thinner in comparison to the 14.41 μm films, with the exception of the (+1-1S-1D) sample. This could be attributed to the differences in surface energies of the alginate films. The higher polarity (due to the presence of carboxyl and hydroxyl groups on the alginate, Figure 4-1) of the 14.41 μm alginate film could prevent the dielectric and silver inks from spreading consequently producing a thicker ink film.

Due to edge effects, the thicknesses of the single and multilayer films were difficult to measure. As shown in Figure 4-7, the thicknesses of the printed layers were thinner at the edges, where more spreading occurred. This can be seen in both

the image on the left showing by color the change in topography, and on the right where the slope of the line decreases from left to right. The high magnification of the Bruker GT-K objective (only a 50 x objective was available for use) also increased the difficulty of this measurement by minimizing the area of view to approximately 1.25 mm by 0.9 mm.

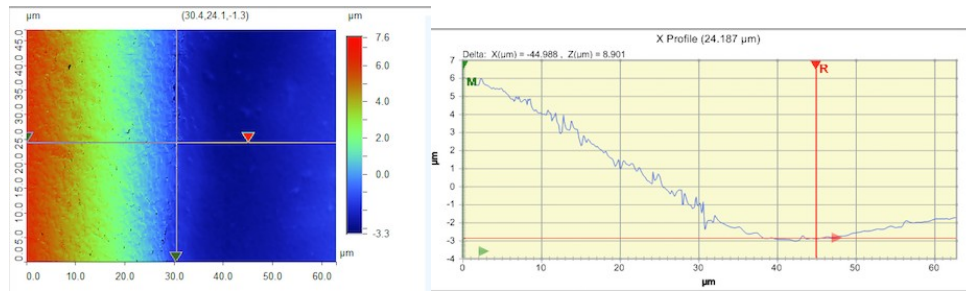


Figure 4-7. Thinning at edges of -1D ink on +1 alginate layer due to spreading

The sheet resistivities of the silver printed layers are shown in Figure 4-8. All measurements were made on PET.

Influence of Alginate and Ag Ink Layer Thickness of Sheet Resistivity

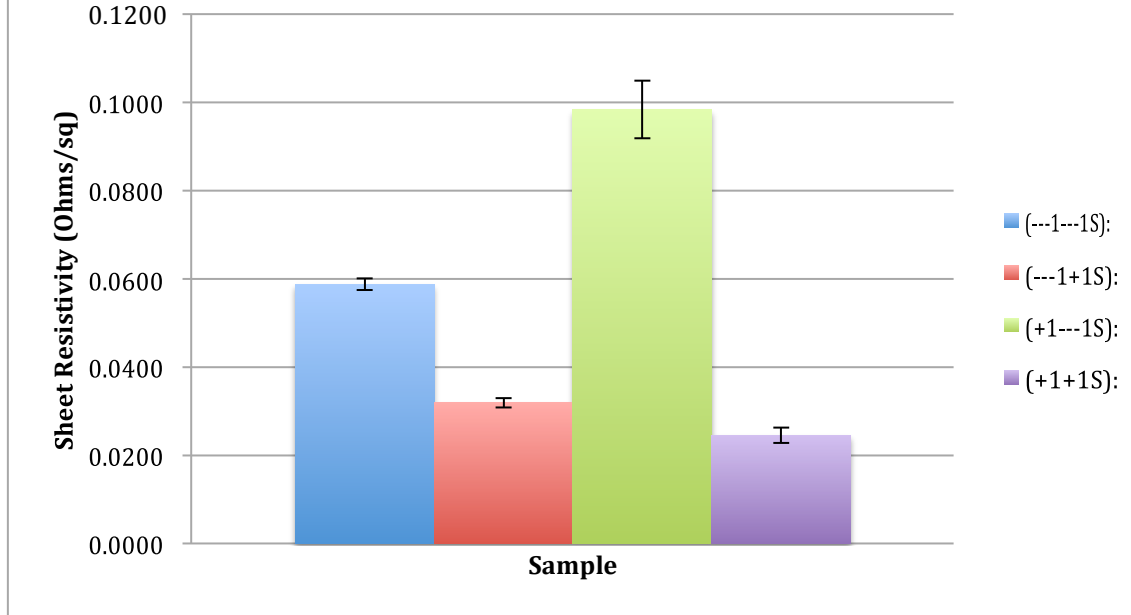


Figure 4-8. Changes in sheet resistivity of single and double printed silver ink layers as a result of altering the thickness of the sacrificial alginate coating layer

Figure 4-9 shows the importance of reporting sheet resistivity versus resistance. The large standard deviations in Figure 4-8 show the unreliability of this test method. The bulk resistivities of the samples are shown in Figure 4-9. Bulk resistivity (e.g. units Ohm-cm) accounts for the thickness of the ink film within its calculation, while resistance does not. It does this by multiplying the resistance by the thickness, giving a resistance times length. The performances of the thicker ink films are significantly better due to the additional thickness. For this reason, the sheet resistivities of the double layer silver samples are lower than the single layer samples. The thickness of the alginate layer had a greater effect on the sheet resistivity of the thinner silver film than the thicker silver film.

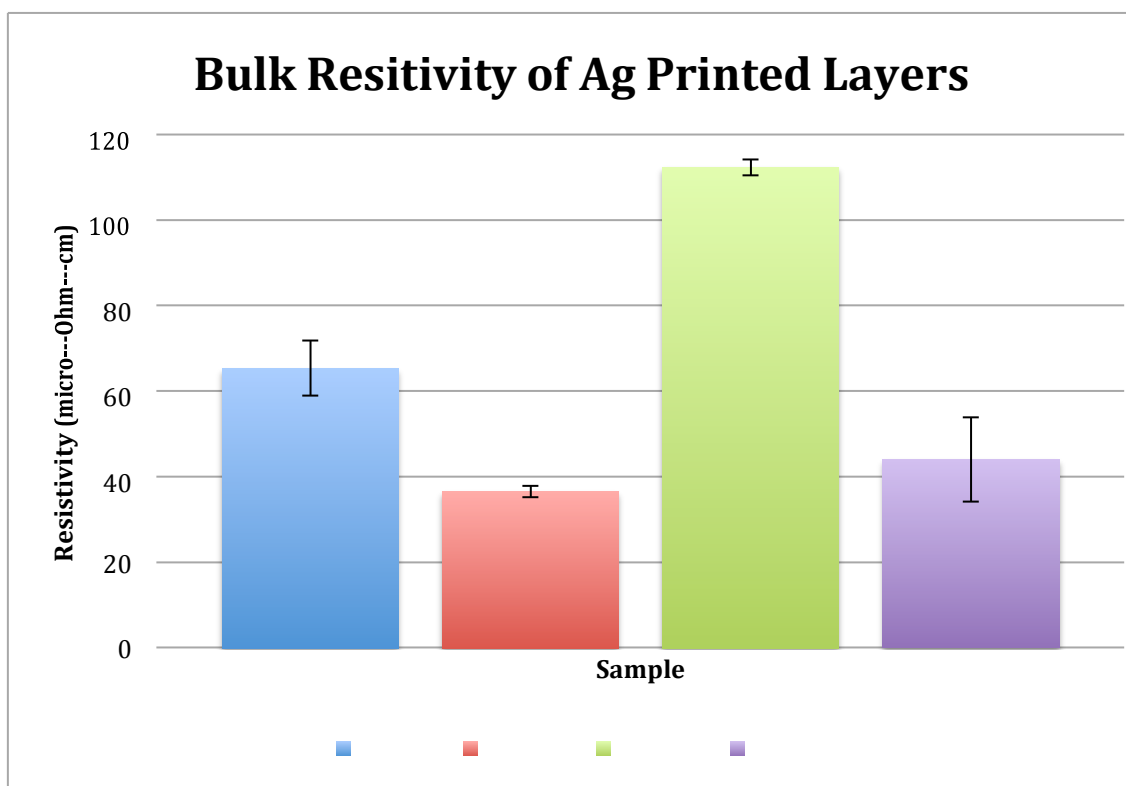


Figure 4-9. Change in Bulk Resistivity of single and double printed Ag over alginate layers of varying thicknesses

As seen in Figure 4-10, the dielectric constants are lower for the ink films lifted-off the thinner alginate coated PET samples, in comparison to the dielectric film printed on the thicker alginate sample. The +1+1D sample was not reported, as the data points were erroneous.

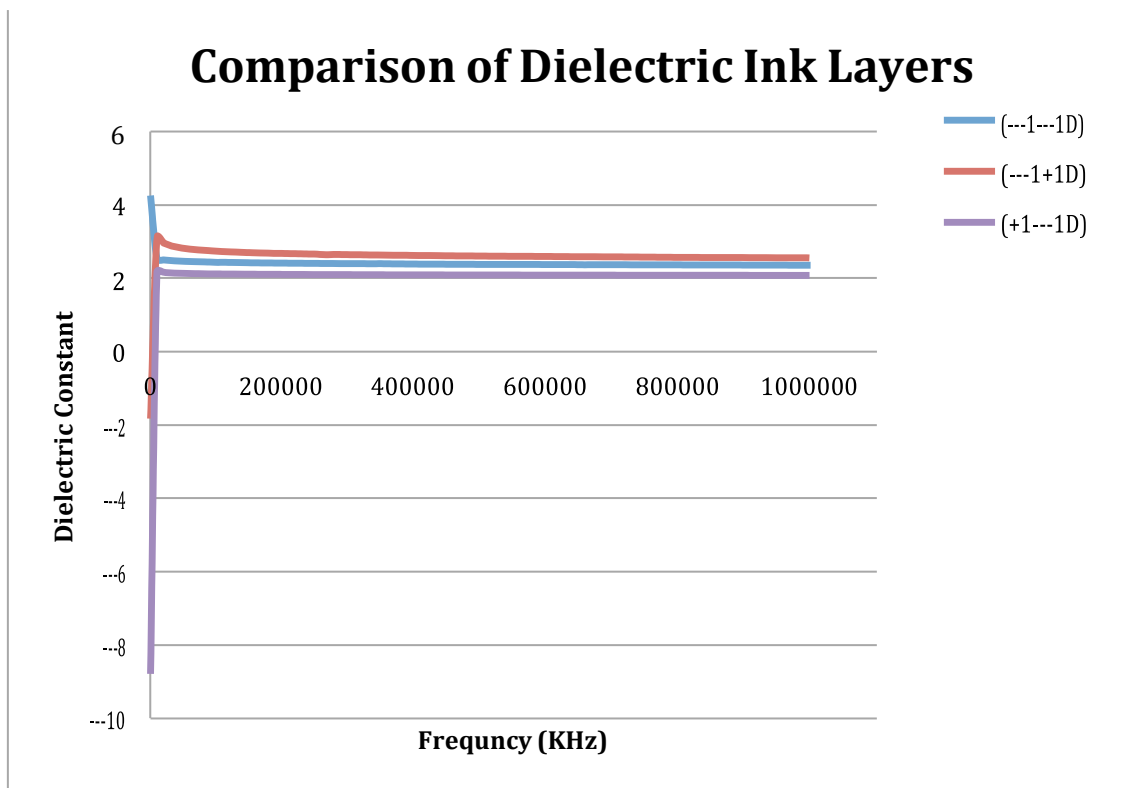


Figure 4-10. Comparison of the dielectric constants of single and double layer printed dielectric ink layers over alginate films of varying thicknesses

Attempts to measure the influence of flexing on the electrical properties of the film using the Mark-10 failed, due to the low mechanical strength of the self-supported films. The samples could not be clamped into the test equipment without tearing or wrinkling. Gurley stiffness measurements were also attempted using a 5 gram weight, placed in the secondary position of the pendulum. Attempts made to measure the single and multi-layered self-supported films failed because the films were too flexible to attain an accurate measurement and too weak to be properly clamped into the instrument without tearing or wrinkling. Attempts were also made to measure the stiffness of the single and multi-layered printed films on alginate films peeled off the PET, as well as, samples while still on the PET. Attempts to make measurements on the alginate films peeled off the PET failed due the sticking of the films to the instrument pendulum. While those measured on the PET exceeded the maximum measureable stiffness.

Attempts to measure the tensile strength of the self-supported films and films peeled off the PET with an Instron tensile tester were also not successful. Once again, the self-supported samples were too weak to survive being mounted onto the instrument. Attempts to measure the alginate printed films peeled off the PET failed due to the alginate stretching past the breaking point of the ink films, meaning the tensile strength of the alginate films exceeded that of the ink films.

Ink film densities were able to be determined after removal of the films from the PET. Figure 4-11 shows the results obtained by measuring the weight and caliper of the samples, of known dimensions. From Figure 4-11 it may be seen that the density of the second layer is higher than that of the first layer (for both the silver and dielectric inks). This could be due to an incomplete removal of solvents in the first layer, or due to inaccuracies of the thickness measurements incurred by the edging effects. By having solvent left in the first layer prior to drying of the second layer the second layer during curing acts as a solvent trap on the solvents trying to escape from the first layer. If the same percentage of solvent was removed, all the silver films would have the same density and all the dielectric films would have the same density.

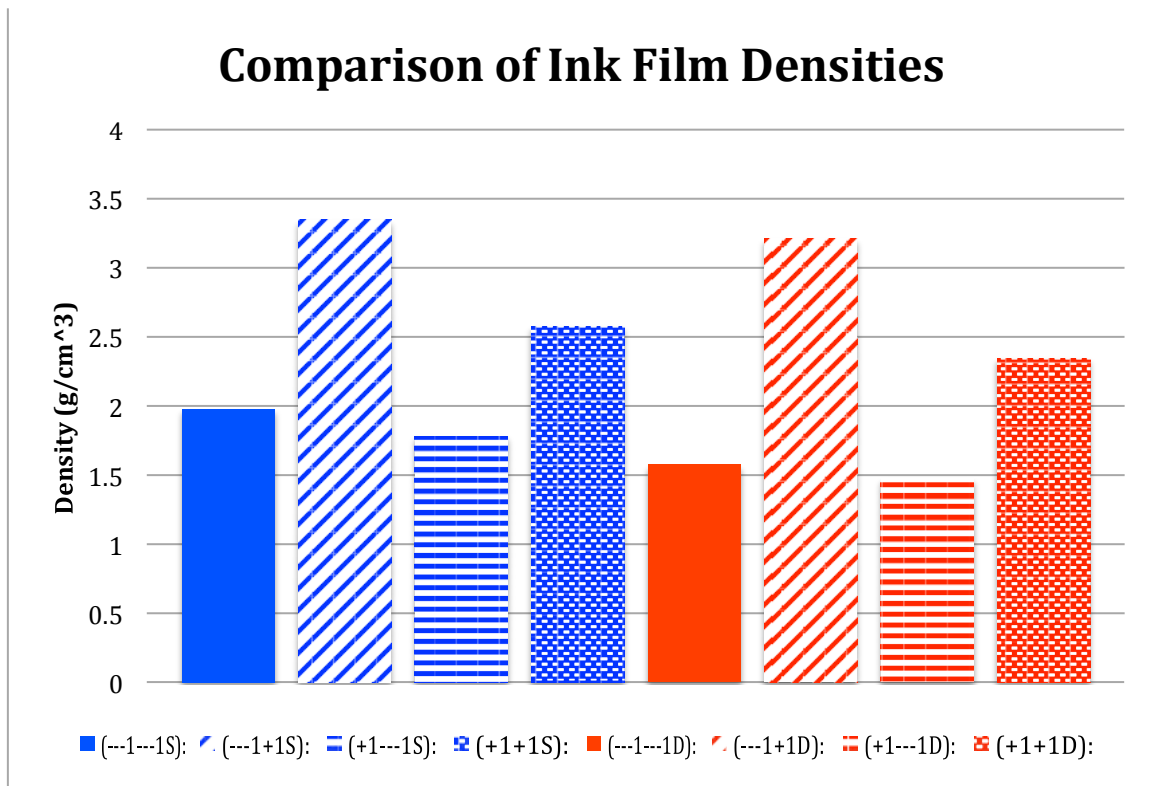


Figure 4-11. Changes in ink film density resulting from the printing of a second Ag and dielectric layer

Figures 4-12 and 4-13 show a comparison of the top and backsides roughness of the self-supported silver ink films. As shown, the roughness of the topside that was not in contact with the PET film is nearly twice as rough as the side of the film, which was in direct contact with the PET.

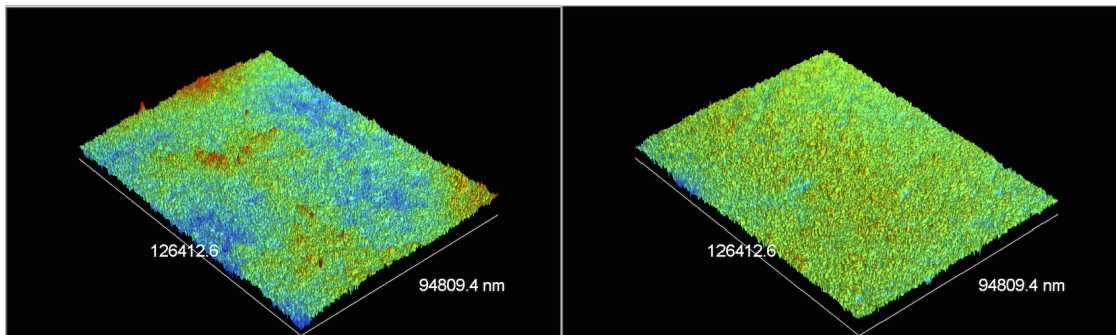


Figure 4-12. -1+1S Top Side (Sa=0.74u)

Figure 4-13. -1+1S Bottom Side (Sa=0.342um)

Similar differences can be seen between the topside and backside for all the silver films in Figure 4-14.

The difference in surface topography of the top and bottom surface of the films is attributed to the difference in the smoothness of the surfaces in which they are in contact. That is, the topside is the side that contacts the printing screen, which is highly rough due to the mesh openings, as well as being exposed to the particulate matter within the environment during drying. In comparison, the bottom side of the ink film is in direct contact with the highly smooth (in relation to the printing screen) alginate coated PET film, and is protected from the environment during drying. This difference in roughness is apparent when looking at the differences between the top and bottom S_a statistical values. The S_a value depicts the average roughness averaged over an area (a 3D parameter).^{55,56,57} The differences in topography of the top and bottom side of the silver ink films shows an approximate 50% reduction in S_a values.

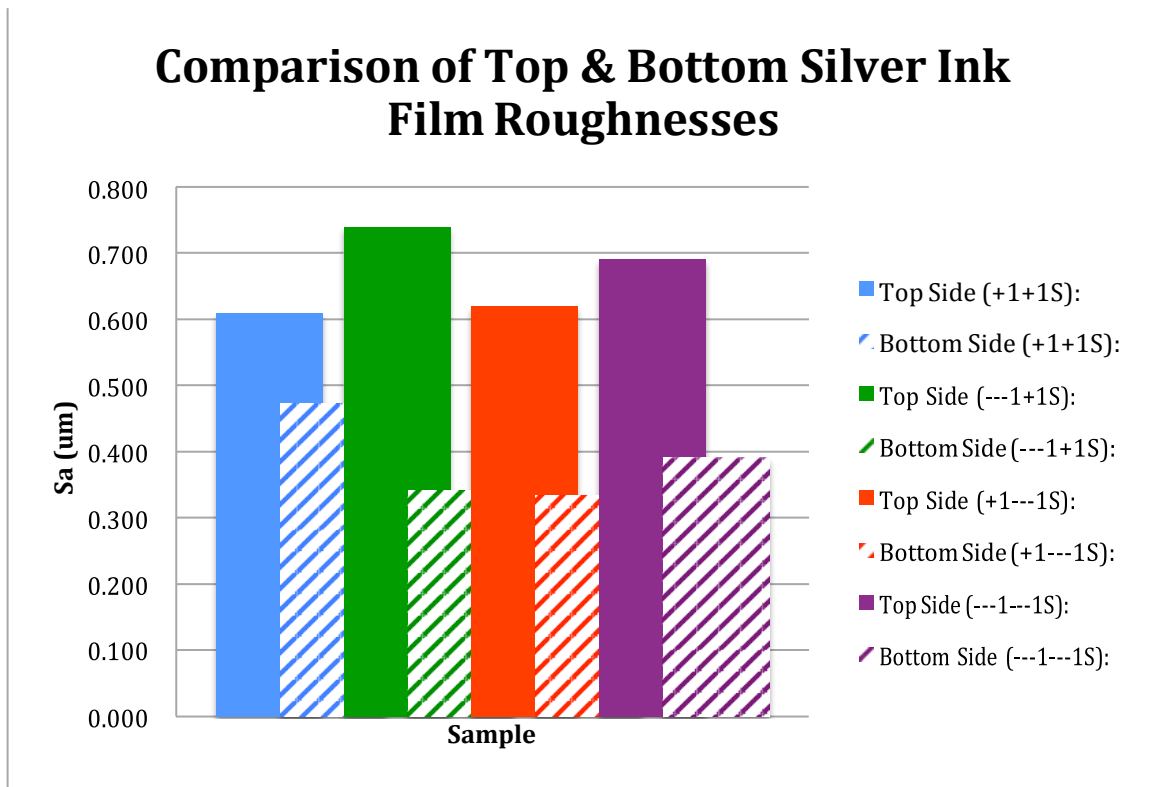


Figure 4-14. Ability to produce highly smooth ink films by use of novel lift-off process to obtain self-supported ink films

One of the main objectives of this research was to determine if the self-supported films (combined to create a capacitor) could be rolled without damage to

the ink layers, and capacitor itself. This objective was successfully achieved. A single stacked capacitor was successfully rolled without damage, as seen in Figure 4-15 below. The gain in device flexibility, as a result of not having a carrier substrate layer is obvious. These encouraging results show promise for the use of this technology as a means to produce a supercapacitor by rolling a multi-stacked device or to minimize the size of a device to fit into tight places.

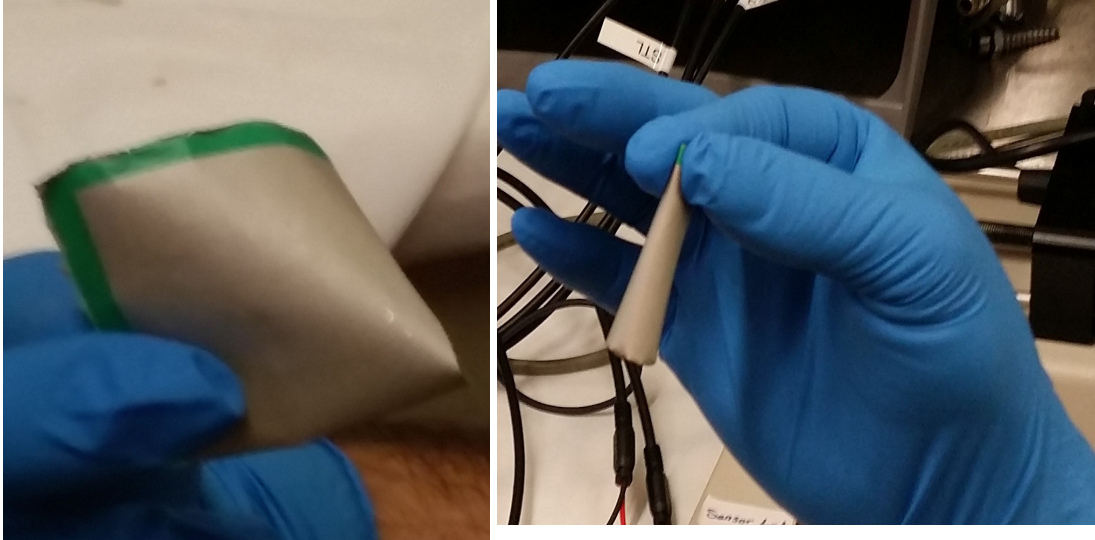


Figure 4-15. Self-supported Rolled Capacitor

CONCLUSIONS

A process to produce self-supported electrically functional ink layers was demonstrated. Smooth alginate films (sacrificial substrates) were produced by casting a 6% solution of alginate containing 20% glycerol on weight of alginate onto a PET substrate. This film served as a sacrificial layer for enabling the lift-off of screen-printed thermal silver and UV dielectric ink films from a PET film after immersion of the printed samples in distilled water. The thickness of the alginate film was found to influence the thickness of the printed dielectric and silver layers, which impacted their electrical performance. The ability to produce self-supported films to determine the dielectric constant of a dielectric ink film at different thicknesses was demonstrated. This is further supported by the fact that the final dielectric measurement of 3.81 (dielectric constant), calculated from the final capacitance

measurements (from the fully printed capacitor) was within range of what the manufacturer reported (which is about 4). This was also true for the silver inks' sheet resistivity measurements, which was reported as being between 0.015-0.020 Ohms/sq/mil. The finding of the differences from the top to bottom side silver roughness is of great interest. The ability to use the bottom side of a printed layer for use when high smoothness is required may prove to be valuable. The density measurements also proved to be highly useful when calculating for the bulk resistivity and will be highly useful for any situation where accurate densities need to be accomplished. The ability to roll single stacked layer capacitor was demonstrated and holds promise for the creation of supercapacitors by this technique.

Recommendations for Future Studies

In order to be able to measure the mechanical properties of the self-supported films, it is recommended that much thicker ink layers (approximately 3-5 times thicker) be printed. A larger print pattern should also be printed to enable multiple strips to be cut from the same sample for testing. Further studies should be performed with different silver ink chemistries. Nano and flake water based inks applied by various print methods should be studied to determine if self-supported ink films can be produced from the same lift-off process by use of non-water soluble gums and resins. The measurement of ink film thicknesses should be accomplished using a smaller magnification objective allowing for more of the printed ink film to be viewed while testing. This should allow for more accurate measurement of the ink film thicknesses. It is also recommended that the Bruker instrument be equipped with a porous stone vacuum table allowing the samples to be held flatter to the surface (as many of the samples displayed some curl, which required them to be taped that was destructive to the samples). Creation of the alginate films should be accomplished in the confines of clean room to prevent the inclusion of particulate matter, which could cause pin holing if thinner layers are printed. For the same reasons, printing should also be performed in a clean room environment. In future studies, the addition of one dielectric layer should be added to either the top or bottom side of the capacitor

allowing for electrical properties to be measured while the device is rolled in order to see if this method would be useful as a means for producing a multi-stacked supercapacitor.

REFERENCES

- ¹ Pech, D., Brunet, M., Taberna, P.L., Simon, P., Fabre, N., Mesnilgreuter, F., Conedera, V., Durou, H., “Elaboration of a Microstructured Inkjet-Printed Carbon Electrochemical Capacitor”, *J. Power Sources*, p. 1266, (2010).
- ² Kang, J.Y., “Micropower for Medical Application, in: J.G. Webster (ed.), *Encyclopedia of Medical devices and Instrumentation*, Wiley, (2006).
- ³ Kaempgne, M., Chan, C.K., Ma, J., Cui, Y. and Gruner, G., “Printable Thin film Supercapacitors Using Single-Walled Carbon Nanotubes,” *Nano Letters*, vol. 9, no. 5 p. 1872, (2009).
- ⁴ Miller, J.R., Simon, P., *Science* 321, pp. 651-652, (2008).
- ⁵ Simon, P., Gogotsi, Y., *Nat. Mater.*, pp. 845-854, (2008).
- ⁶ Kaempgen, M., Ma, J., Gruner, G., Wee, G., Mhaisalkar, S.G., *Appl. Phys. Lett.*, 90, pp. 264104-264106, (2007).
- ⁷ Kiebele, A., Gruner, G., *Appl. Phys. Lett.* 91, pp. 144104-144107, (2007).
- ⁸ Grande, L., Chundi, V.T., Wei, D., Bower, C., Andrew, P., Ryhanen, T., “Graphene for Energy Harvesting/Storage Devices and Printed Electronics”, *Particuology*, 10, pp. 1-8, (2012).
- ⁹ Swanson, R. M., “Photovoltaics Power Up”, *Science*, Vol. 324 15, pp. 891-892, (2009).
- ¹⁰ Sterken, T., Fiorini, P., Van Hoof, C., and Puers, R., “A Hybrid Electrodynamical Vibration Harvester”, *Proceedings of Power MEMS*, pp. 85-88, (2007).
- ¹¹ Challa, R.V., Prasad, M.G., Shi, Y., and Fisher, F.T., “A vibration energy harvesting device with bidirectional resonance frequency tenability”, *Smart Mater. Struct.*, 17 015035 (2008).
- ¹² Linden, D., *Handbook of batteries and fuel cells*, second edition, McGraw-Hill, (1995).
- ¹³ William Fortune Smith and Javad Hashemi, *Foundations of materials science and engineering*, (4th edition), McGraw-Hill, (2006).
- ¹⁴ Ruddell, A., “Storage Technology Report, ST6: Flywheel”, (2003).
- ¹⁵ Jog, M.G., *Hydroelectric and pumped storage plants*, Halsted Press, New York, NY, (1989).
- ¹⁶ Jiang, Z., “Assessment and Market Analysis of Solid State Ultracapacitors”, Masters Thesis, MIT, September (2007).
- ¹⁷ Bird, J., (2010), *Electrical and Electronic Principles and Technology*. Routledge. pp. 63–76, (retrieved 2013-07-5).
- ¹⁸ Jayalakshmi, M., Balasubramanian, K., “Simple Capacitors to Supercapacitors-An Overview,” *Int. J. Electrochem. Sci.*, 3, pp. 1196-1217, (2008).
- ¹⁹ Halper, M.S., Ellenbogen, J.C., “Supercapacitors: A Brief Overview,” MITRE, pp. 1-41, (2006).
- ²⁰ Butler, P., Miller, J.L. and Taylor, P.A., “Energy Storage Opportunities analysis Phase II Final Report, A Study for the DOE Energy Storage Systems Program”, Sandia Report, Sandia National Laboratories, p. 16, (2012).

-
- ²¹ Winter, M., & Brodd, R.J., "What are batteries, fuel cells, and supercapacitors?" *Chemical Reviews*, 104 (10), 4245-4270.
- ²² Helmholtz, H. von, *Ann. Phys. (Leipzig)*, vol. 89 p. 211 (1853).
- ²³ Hsueh, C.H., Ferber, M.K., *Composites Part A*, 33,, p.1115, (2003).
- ²⁴ Pollet, M., Marinel, S., Desgardin, G., J., *Euro. Cera. Soc.*, p. 119, (2004).
- ²⁵ Jayalakshmi, M., Balasubramanian, K., *Int. J. Electrochem. Sci.*, 3, p. 1202-1210, (2008).
- ²⁶ Nagata, H., Won Ko, S., Hong, E., Randall, C.A. and McKinstry, S.T., "Microcontact Printed BaTiO₃ and LaNiO₃ thin Films for Capacitors," *J. Am. Ceram. Soc.*, 89, p. 2816, (2006).
- ²⁷ Keskinen, J., Sivonen, E., Jusso, S., Bergelin, M., Johansson, M., Vaari, A., Simolander, M., "Printed Supercapacitors on Paperboard Substrate," *Electrochimica Acta*, 85, pp. 302-306, (2006).
- ²⁸ Lim, J., Kim, J., Yoon, Y.J., Kim, H., Yoon, H.G., Lee, S-N, Kim, J., "All-Inkjet Printed Metal-Insulator-Metal (MIM) Capacitor," *Current Applied Physics*, 12, pp. e14-e17, (2012).
- ²⁹ Le, L.T., Ervin, M.H., Qiu, H., Fucjs, B.E., Zumino, J., and Lee, W.Y., "Inkjet-Printed Graphene for Flexible Micro-Supercapacitors," 11th International Conference on nanotechnology, Portland WA, August 15-18, pp. 67-71, (2011).
- ³⁰ Hartman, A., Clemson University MS thesis, "Printing Carbon Nanotube Based Supercapacitors for Packaging," (2011).
- ³¹ Nair, R.B., Grigorenko, P., Novoselov, A., Booth, K., Stauber, T., et al. "fine structure constant defines visual transparency of graphene," *Science*, 320 (5881), p. 1308, (June 6, 2008).
- ³² Blake, P., Brimicombe, P., Nair, R., Booth, T., Jiang, D., Schedin, F., et al., "Graphene-based liquid crystal device," *Nano Letters*, 8 (6), pp. 1704-1708
- ³³ Liu, C., Yu, Z., Neff, D., Zhamu, A., & Jang, B.Z., "Graphene-based supercapacitor with an ultrahigh energy density," *Nano Letters*, 10, pp. 4863-4868, (2012).
- ³⁴ Wang, Y., Shi, Z., Huang, Y., Ma, Y., Wang, C., Chen, M., et al., "Supercapacitor device based on graphene materials," *The Journal of Physical Chemistry C*, 113(30), pp. 13103-13107 (2009).
- ³⁵ Yu, A., Roes, I., Davies, A., & Chen, Z., "Ultrathin, transparent, and flexible graphene films for supercapacitor application," *Applied Physics Letters*, 96 (25), p. 253105 (2010).
- ³⁶ Yu, D. & Dai, L., "Self-assembled graphene/carbon nanotube hybrid films for supercapacitors," *The Journal of Physical Chemistry Letters*, 1(2), pp. 467-470, (December 22, 2009).
- ³⁷ Wu, Q., Xu, Y., Yao, Z., Liu, A., & Shi, G., "Supercapacitors based on flexible graphene/polyaniline nanofiber composite films," *ACS Nano*, 4 (4), pp. 1963-1970, (2010).

-
- ³⁸ Han, Y., Ding, B., & Shang, X., "Preparation of graphene/polypropylene composites for electrochemical capacitors," *Journal of New Materials for Electrochemical Systems*, 13, pp. 315-320, (2010).
- ³⁹ Keskinen, J., Sivonen, E., Jusso, S., Bergelin, M., Johansson, M., Vaari, A., Simolander, M., "Printed Supercapacitors on Paperboard Substrate," *Electrochimica Acta*, 85, pp. 302-306, (2012).
- ⁴⁰ Le, L.T., Ervin, M.H., Qiu, H., Fucjs, B.E., Zumino, J., and Lee, W.Y., "Inkjet-Printed Graphene for Flexible Micro-Supercapacitors," 11th International Conference on nanotechnology, Portland, WA, August 15-18, pp. 67-71, (2011).
- ⁴¹ US Patent # 20060105492, Ogier, S.D., Veres, J., Yeates, S.G., (July 30, 2003).
- ⁴² US Patent # 4861425, Greer, S.E., Howard Jr., R.T., (Feb. 28, 1990).
- ⁴³ US Patent# 201001163878, Broer, D.J., Haskal, E.I., McCulloch, D.J., (April 29, 2009).
- ⁴⁴ US Patent # 20100002402, Rogers, J.A., Huang, Y., (Dec. 1, 2010).
- ⁴⁵ E. Zeria, IdTechEx Printed Electronics USA Conference Presentation, San Francisco, CA, (2007).
- ⁴⁶ Western Michigan University Printed Electronic Short Course, Erika Rebrosova, Deposition Methods, (2011).
- ⁴⁷ Ingram, S., *Screen Printing Primer*, GATF Press, 2nd Ed., Sewickley, PA, (1999), pp. 1- 2.
- ⁴⁸ Ingram, S., *Screen Printing Primer*, GATF Press, 2nd Ed., Sewickley, PA, (1999), pp. 45-48.
- ⁴⁹ Faine, B., *The Complete Guide to Screen Printing*, North Light Books, Cincinnati, OH, (1989).
- ⁵⁰ Ingram, S., *Screen Printing Primer*, GATF Press, 2nd Ed., Sewickley, PA, p. 57, (1999).
- ⁵¹ http://www.fusionuv.com/uv_bulbs.aspx.
- ⁵² <http://www.firsttenangstroms.com/pdfdocs/OwensWendtSurfaceEnergyCalculation.pdf>.
- ⁵³ Owens, D. K. and Wendt, R. C. Estimation of Surface Free Energy of Polymers. *s.l. j. Appl. Polym. Sci*, 13, pp. 1741-1747, (1969).
- ⁵⁴ <http://www.visit-alginate.com/sodium-alginate-chemical-properties.html>, (2014).
- ⁵⁵ http://www.olympus-ims.com/en/knowledge/metrology/roughness/3d_parameter/, (2014).
- ⁵⁶ www.bruker.com/%2Fnc%2Fproducts%2Fsurface-analysis%2F3d-optical-microscopy%2Fcontourgtk%2Flearnmore.html%3Fcid%3D44106%26did%3D39905%26sechash%3Dfcf7f177&ei=xme1U5LIDtWkyASs8oHIAg&usg=AFQjCNG3B2u6jVZc2ShreG8f9cYH93SNsQ&sig2=wpc128bqTO3WpldEyQrtcA
- ⁵⁷ https://www.bruker.com/fileadmin/user_upload/8-PDF-Docs/SurfaceAnalysis/AFM/Webinars/Bruker-SlidingFriction-presentation-07262013.pdf